Journal of the Korean Institute of Illuminating and Electrical Installation Engineers (2011) 25(7) : 97~104
DOI : 10.5207/JIEIE.2011.25.7.097

논문 25-7-14

Modeling and Control of IGBT Converter-Based High-Voltage Direct Current System

Hong-Woo Kim* · Suk-Whan Ko · Hae-Joon An · Gil-Soo Jang · Hee-Sang Ko**

Abstract

This paper presents modeling and control for the emerging IGBT converter-based high-voltage direct-current system (IGBT-HVDC). This paper adds to the representation of the IGBT-HVDC system in the dq-synchronous reference frame and its decoupled control scheme. Additionally, since the IGBT-HVDC is able to actively support the grid due to its capacity to control independently active and reactive power production, a reactive power control scheme is presented in order to regulate/contribute to the voltage at a remote location by taking into account its operational state and limits. The ability of the control scheme is assessed and discussed by means of simulations using ahybrid power system, which consists of a permanent magnetic synchronous-generator (PMSG) based wind turbine, an IGBT-HVDC, and a local load.

Key Words : Control, High-Voltage Direct Current(HVDC), Permanent-Magnetic Synchronous-Generator (PMSG), Wind Turbine

1. Introduction

HVDC technology finds applicationsin the transmission of power over long distances, significant underwater distances, and in the interconnection of separate alternating current (ac) systems [1]-[3]. These systems have a long history and are likely to continue to be used in the future, especially as technological improvements make them competitive cost-wise with alternative acschemes. Their unique control characteristics can be exploited to enhance the capacity and level of interconnection of existing ac systems.

HVDC systems have been undergoing research and development for many years in areas such as the Middle East, China, India and South America as they require infrastructure to power their growth. Power sources in these places were based initially on thyristor technology and more recently on

* Main author : Wind Energy Center, Korea Institute of Energy Research
** Corresponding author : Product Development Team/Wind Turbine Division, Samsung Heavy Industries Company
Tel : +82-42-860-3412, Fax : +82-42-860-3543
E-mail : heesangko@gmail.com
Date of submit : 2011. 5. 25
First assessment : 2011. 6. 8
Completion of assessment : 2011. 7. 14

fully-controlled semiconductors and voltage-source converter (VSC) topologies [4]-[14]. The ever-increasing penetration of power electronics technologies into the power systems is mainly dueto the continuous progress of high-voltage high-power fully-controlled semiconductors. The fully-controlled semiconductor devices available today for high-voltage high-power converters are either thyristors or transistors.

Today, there are more than 92 HVDC projects worldwide transmitting more than 75GW of power using two distinct technologies as follows [14]: a) line-commutated current-source converters using thyristors, a technology that is well established for high power, typically around 1000MW, with the largest project being the Itaipu system in Brazil at 6300MW power level [14], and b) forced-commutated VSCs using gate-turn-off thyristors or, in most industrial cases, insulated gate-bipolar-transistors (IGBTs). It is well established technology for medium power levels with the largest size project being the latest one named Cross Sound Cable in the North Eastern USA at 1000 MW level [14]-[26].

Since recent emerging technologies in the application of VSC-HVDC enable the use of pulse-width-modulation (PWM) and IGBT [26], VSC-HVDC can provide rapid, independent control of active and reactive power [27], small contributions to short circuit currents [28], the feed of remote isolated loads from a main ac grid [29],and enhanced power quality [30].

Hence, it is important to develop proper tools and models to fully realize the advantages of IGBT-HVDC. With this in mind, this paper presents a dq-synchronous reference frame [31] representation of the IGBT-HVDC system and its decoupled control scheme. As a result, the proposed model and control scheme can be easily utilized to power system models and stability analyses.

This paper is organized as follows: The modeling of an IGBT-HVDC system is presented in section II, in section III and IV, a decoupled control scheme and a reactive power control method are described, the simulation result isshown in section V, and concluding remarks are given in section VI.

2. Modeling of an IGBT-HVDC System

Fig. 1 shows the study system, which consists of a permanent-magnetic synchronous-generator (PMSG) wind turbine, a local load, and an IGBT-HVDC. An IGBT-HVDC system is realized through IGBT-HVDC links, transformers (TR), and six-pulse converter bridges. The model of the PMSG used in this paper is from [32]. The mathematical models of the electrical components such as a TR, a transmission line (TL), and a local load can be found in [33].

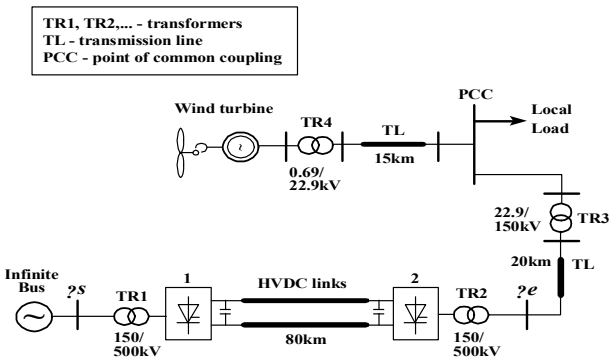

Fig. 1. Grid-connected ac hybrid power system

The representation of an IGBT-HVDC system is evaluated as shown in Fig. 2 using a resistance R_1, a reactance L_1, and a capacitance C_c. The capacitance C_o is fabricated for modeling purposes and is set to 10^{-6} in per unit.

The dq-axes models of Fig. 2 are represented as

shown in Fig. 3, and their corresponding equations are followed in Eq. 1 and Eq. 2. In Fig. 3, the voltages $^{\mathbf{v}}dq11$ and $^{\mathbf{v}}dq31$ are obtained from the voltages $^{\mathbf{v}}dq,r1$ and $^{\mathbf{v}}dq,i1$ by multiplying the converter control signals that are depicted in Fig. 4 and Fig. 5. In this paper, the power electronic converters are represented using average-value models that are expressed in the dq-synchronous reference framesas given in [31].

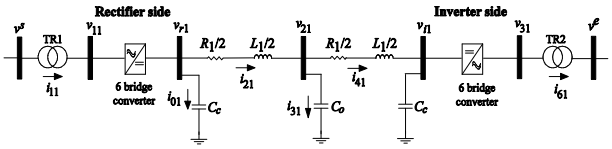

Fig. 2. One line diagram of the IGBT-HVDC system

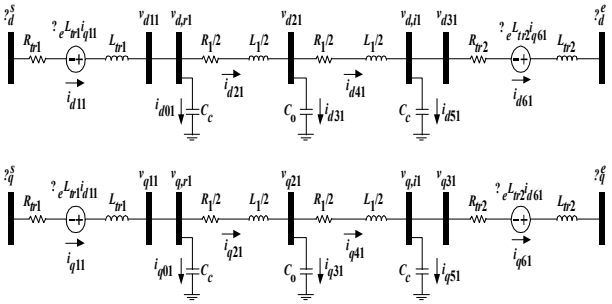

Fig. 3. The dq-synchronous reference frame representation of the IGBT-HVDC system (top: d-axis, bottom: q-axis)

$$v_d^s - v_{d11} = R_{tr1} i_{d11} - \omega_e L_{tr1} i_{q11} +$$

$$v_{d,r1} - v_{d21} = \frac{R_1}{2} i_{d21} + \frac{L_1}{2\omega_b} \frac{di_{d21}}{dt}$$

$$i_{d21} - i_{d41} = \frac{c_o}{\omega_b} \frac{dv_{d21}}{dt}$$

$$v_{d21} - v_{d,i1} = \frac{R_1}{2} i_{d41} + \frac{L_1}{2\omega_b} \frac{di_{d41}}{dt}$$

$$v_{d31} - v_d^s = R_{tr2} i_{d61} - \omega_e L_{tr2} i_q 61 \cdot$$

$$i_{d11} - i_{d21} = \frac{C_c}{\omega_b} \frac{dv_{d,r1}}{dt}$$

$$i_{d41} - i_{d61} = \frac{C_c}{\omega_b} \frac{dv_{d,i1}}{dt}$$

$$v_q^s - v_{q11} = R_{tr1} i_{q11} - \omega_e L_{tr1} i_{d11} +$$

$$v_{q,r1} - v_{q21} = \frac{R_1}{2} i_{q21} + \frac{L_1}{2\omega_b} \frac{di_{q21}}{dt}$$

$$i_{q21} - i_{q41} = \frac{c_o}{\omega_b} \frac{dv_{q21}}{dt}$$

$$v_{q21} - v_{q,i1} = \frac{R_1}{2} i_{q41} + \frac{L_1}{2\omega_b} \frac{di_{q41}}{dt}$$

$$v_{q31} - v_q^s = R_{tr2} i_{q61} - \omega_e L_{tr2} i_d 61 \cdot$$

$$i_{q11} - i_{q21} = \frac{C_c}{\omega_b} \frac{dv_{q,r1}}{dt}$$

$$i_{q41} - i_{q61} = \frac{C_c}{\omega_b} \frac{dv_{q,i1}}{dt}$$

3. The Decoupled Control Scheme of the IGBT-HVDC

IGBT converter controls have several advantages over thyristor converter controls. These include avoidance of commutation failures due to disturbances in the ac network, independent control of the reactive and active power consumed or generated by the converter, the possibility to connect an IGBT-HVDC system to a weak ac network or even to one where no generation source is available and the short-circuit level is naturally very low, and a faster dynamic response due to higher than the fundamental switching frequency operation, which further results in reduced need for filtering and hence smaller filter size. For these reasons, several IGBT-HVDC systemshave been commissioned in recent years, including the connection of off-shore wind farms or oil drilling platforms into the mainland electrical network and for underground transmission or distribution systems within densely-populated cities [14], [15].

However, to fully utilize the advantages of an IGBT-HVDC system,a properly designed control

system is essential. To develop a control plan, it is assumed that the rectifier-side converter controls the active-current set-point, which is controlled by the dc-voltage v_{r1}, and the reactive-current set-point, which is set to zero for the unity power factor (or power factor control, PFC). The inverter-side converter works to control the active-current set-point, and the reactive-current set-point, which is also set to zero for the PFC.

The decoupled control scheme is then finalized as depicted in Fig. 4 for the rectifier-side and in Fig. 5 for the inverter-side with the corresponding de-coupling terms $\omega_e L_{tr2}\mathbf{i}_{dq21}$ and $\omega_e L_{tr2}\mathbf{i}_{dq41}$ between the d and qaxis. Subscripts r and i stand for the rectifier- and the inverter-side, respectively. In Fig. 4, the voltage v_{r1}^{set} is the dc-voltage set-point, and the measured voltage v_{r1} can be obtained by $v_{r1}=\sqrt{v_{d,r1}^2+v_{q,r1}^2}$. The current set-point i_{d21}^{set} to the rectifier-side control is set to zero for the PFC, and the current set-points to the inverter-side control are computed by

$$\begin{bmatrix} i_{d41}^{set} \\ i_{q41}^{set} \end{bmatrix} = \begin{bmatrix} v_{d,i1} & v_{q,i1} \\ v_{q,i1} & -v_{d,i1} \end{bmatrix}^{-1} \begin{bmatrix} P_{i1}^{set} \\ Q_{i1}^{set} \end{bmatrix} \quad (3)$$

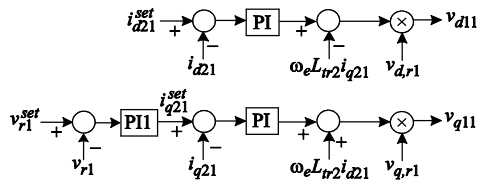

Fig. 4. Block diagram of the rectifier-side control in the IGBT-HVDC system

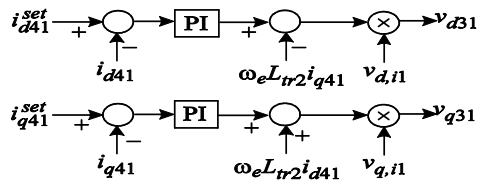

Fig. 5. Block diagram of the inverter-side control in the IGBT-HVDC system

4. The Reactive Power Control

As shown in Fig. 5, Converter 2 (inverter-side, see Fig. 1) operates conventionally in the PFC. A reactive power control scheme is presented in this section. The purpose of the reactive power control is to regulate the voltage at a specified remote PCC (see Fig. 1) by adjusting the reactive power produced by the converter 2 of the IGBT-HVDC (see Fig. 1), taking into account its operating state and limits. As depicted in Fig. 6, the control objective is to utilize Q_{i1} from Converter 2 of the IGBT-HVDC to control the voltage at the PCC to the predefined value by the reactive power set-point control signal Q_{i1}^{set} (see Eq. 4).

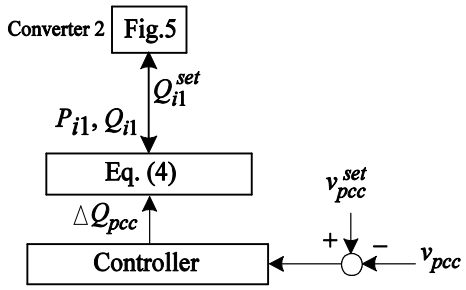

Fig. 6. Schematic diagram of the reactive power control

When controlling the converter, it is important that the operating limit of the converter is not exceeded. By considering the operating limits the reactive power required from Converter 2 can be computed as

$$Q_{i1}^{set} = \min\left\{Q_{i1}^{\max},\ Q_{i1}^{\max}\Delta Q_{pcc}\right\} \quad (4)$$

where $Q_{i1}^{\max}$ is the maximum available reactive power (limit) that Converter 2 can provide, and ΔQ_{pcc} is the total reactive power required to support the voltage at the PCC.

Fig. 7shows the active- and the reactive-power

operating limits, wherein it is assumed that Converter 2 should not exceed its apparent power limit $S_{i1}^{\max}$ depicted by the half-circle. The maximum available reactive power from Converter 2 can then be expressed as

$$Q_{i1}^{\max} = \sqrt{\left(S_{i1}^{\max}\right)^2 - P_{i1}^2} \quad (5)$$

where it is assumed that the nominal apparent power of the converter is $S_{i1}^{\max}$, defined here as the converter rating. Based on Fig. 7, it also follows that $-S_{i1}^{\max} \le P_{i1} \le S_{i1}^{\max}$.

Suppose that at a given time, a converter is delivering active power as denoted herein by P_{i1}. Then, in addition to the active power, the converter can supply or absorb a maximum of $Q_{i1}^{\max}$ of the reactive power. Therefore, the reactive power available from the converter lies within the limits $\left[-Q_{i1}^{\max};\ +Q_{i1}^{\max}\right]$, which are operating-condition dependent.

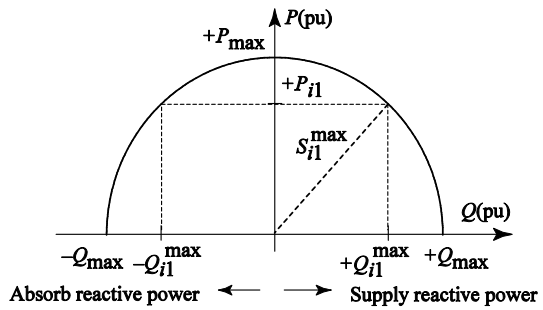

Fig. 7. Converteractive and reactive power operating limits

A proportional-integral (PI) controller is designed for the controller shown in Fig. 6, and its gains are summarized in the Appendix. Since limiting control action should be implemented in tandem with an integrator anti-windup scheme that would stop integrating error when the limit is approached, a PI controller with the proposed distributed anti-windup is implemented in Matlab/Simulink [19] as shown in Fig. 8.

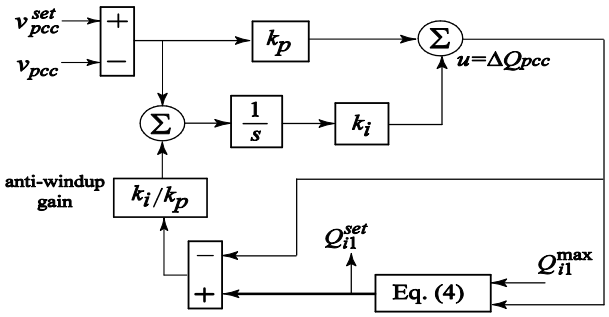

Fig. 8. Implementation of PI controller with the distributed anti-windup

5. Case Studies

The system depicted in Fig. 1 was implemented in detail using the Matlab/Simulink [19]. Computer studies considering the local-load variations, the trip of the wind turbine from the grid, and the three-phase symmetrical fault between the wind turbine and local load were conducted to compare the dynamic responses of the system with different controls. Going forward, Mode 1 indicates the PFC-mode operation of the IGBT-HVDC, which Q_{i1}^{set} is set to zero. As the reactive power control operation, Mode 2 actively utilizes Q_{i1}^{set} for voltage control at the PCC.

A. Local-Load Variation

The local-load impedance was decreased by 20% at $t = 0.2s$. Wind speed is assumed to be 12m/s. The comparison of the voltage transients observed at the PCC is shown in Fig. 9. As noted in Fig. 9, when Mode 1 was in operation, the load impedance changes resulted in a noticeable drop of the bus voltage by 20%,which does not satisfy the permissible voltage range ±2%. When Mode 2 was in operation, voltage recovery to its predefined value

was achieved. Thus, the performance in Mode 2 operation significantly improved the voltage control at the PCC as compared to Mode 1 operation.

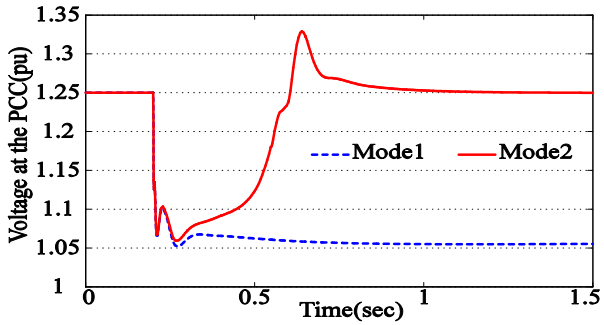

Fig. 9. Voltage observed at the PCC due to local-load variation

B. Wind-Turbine Trip from the Grid

In this study, the wind turbine is disconnected from the grid at $t = 0.2s$. Wind speed is also assumed to be 12m/s. The comparison of the voltage transients observed at the PCC is shown in Fig. 10. As noted in Fig. 10, when Mode 1 was in operation, a noticeable voltage drop at the PCC resulted by 50%, which does not satisfy the permissible voltage range ±2%. When Mode 2 was in operation, voltage recovery to its predefined value was achieved.

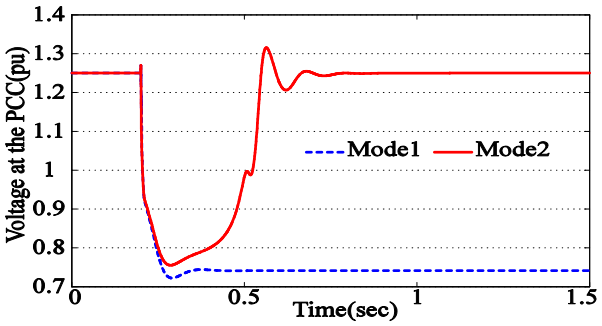

Fig. 10. Voltage observed at the PCC due to the wind-turbine trip

C. Fault in the TL between the Wind Turbine and Local Load

To emulate this scenario, it is assumed that the fault occurred at $t = 0.2s$ and cleared at $t = 0.36s$ in the TL between the wind turbine and local load. Wind speed is 12[m/s]. As noted in Fig. 11, Mode 2 operation resulted in voltage recovery to its predefined voltage at the PCC faster than in the Mode 1 operation.

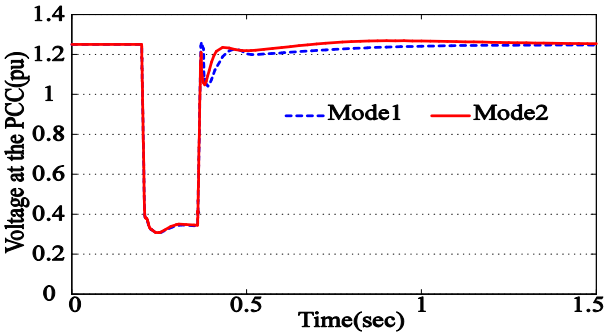

Fig. 11. Voltage observed at the PCC due to the fault

6. Conclusion

This paper proposed a model for the IGBT-HVDC system in a dq-synchronous reference frame and a decoupled control scheme including reactive power control. Since the dq-synchronous reference frame representation of power system models are traditionally used for power system stability analyses, the proposed model representation and its decoupled control scheme can be easily accommodated with power system models for power system stability analyses. The other contribution of this paper is the presentation of a reactive power control methodology. This control scheme takes into account the active power, generated by the converter of the IGBT-HVDC,and ensures that local operating limits are not exceeded. The information passed to the control module is used to calculate the reactive power, required from the converter to achieve the voltage control objective. As shown in simulations, the reactive power control scheme (Mode 2) delivers

improvement in performance as compared to the power factor control scheme (Mode1).

7. Appendix

For simulations, all parameters are converted to per unit based on 2MVA.

Infinite bus voltage, dc-voltage, maximum operating limit of VSC (pu)

$\mathbf{v}_{dq,\inf} = [1.165 \quad 0.185], \quad v_{r1}^{set} = 1.164, \quad S_{i1}^{\max} = 1$

TL and TR parameter connected to IGBT-HVDC (pu)

$R_{TL} = 0.0035, \quad L_{TL} = 0.006, \quad C_{TL} = 0.0004, \quad R_{TR} = 0.02, \quad L_{TR} = 0.3$

IGBT-HVDC and TR(pu)

$R_1 = 0.0055, \quad L_1 = 0.0631, \quad C_c = 0.0109, \quad R_{TR} = 0.0092, \quad L_{TR} = 0.1382$

Controller gains (pu)

- PI: $k_p = 0.5, \quad k_i = 100$ and PI1: $k_p = 4, \quad k_i = 200$
- Reactive power controllers: $k_p = 1, \quad k_i = 20$

References

[1] T. Hasegawa, K. Yamaji, H. Irokawa, H. Shirahama, C. Tanaka, and K. Akabane, Development of a thyristor valve for next generation 500 kV HVDC transmission systems, IEEE Trans. on Power Delivery, 11 (1996) 1783-1788.

[2] L. Ran, D. Xiang, L. Hu, and K. Abbott, Voltage stability of an HVDC systems for a large offshore wind farm with DFIGs, The 8th IEE International Conf. on AC and DC Power Transmission Proc., (2006) 150-154.

[3] M. O. Faruque, Y. Zhang, V. Dinavahi, Detailed modeling of CIGRE HVDC benchmark system using PSCAD/EMTDC and PSB/SIMLINK, IEEE Trans. on Power Delivery, 21(2006) 378-387.

[4] L. Gyugyi, Unified power-flow control concept for flexible AC transmission systems, IEE Part C: Generation, Transmission and Distribution Proc., 139 (1992) 323-331.

[5] L. Gyugyi, Dynamic compensation of AC transmission lines by solid-state synchronous voltage source, IEEE Trans. on Power Delivery, 9(1994) 904-911.

[6] A. A. Edris, S. Zelingher, L. Gyugyi and L. J. Kovalsky, Squeezing more power from the grid, IEEE Power Engineering Review, 22 (2002) 4-6.

[7] E. I. Carroll, Power electronics for very high power applications, ABB Review, 2 (1999) 4-11.

[8] H. Akagi, Large static converters for industry and utility applications, Proc. IEEE Power Engineering Society Summer Meeting Conf. Proc., 89 (2001) 976-983.

[9] T. J. Hammons, M. Willingham, K. N. Mak, M. D. Silva, M. Morozowski, and B. K. Blyden, Generation and transmission improvements in developing countries, IEEE Trans. on Energy Conversion, 14 (1999) 760-765.

[10] A. M. H. A. Karim, N. H. A. Maskati and S. Sud, Status of Gulf co-operation council (GCC) electricity grid system interconnection, IEEE Power Engineering Society General Meeting Proc., 2 (2004)1385-1388.

[11] T. J. Hammons, D. Woodford, J. Loughtan, M. Chamia, J. Donahoe, D. Povh, B. Bisewski, W. Long, Role of HVDC transmission in future energy development, IEEE Power Engineering Review, 20 (2000) 10-25.

[12] L. Weimers, AC or DC: which way should China go? Modern Power Systems, 25 (2005)11-17.

[13] C. Ashmore, Transmit the light fantastic, IET, Power Engineer, 20 (2006) 24-27.

[14] ABB library and references for HVDC [Online] Available: http://www.abb.com/

[15] G. Asplund, K. Eriksson and K. Svensson, HVDC Light DC transmission based on voltage sourced converters, ABB Review, 1 (1998) 4-9.

[16] G. Asplund, K. Eriksson and O. Tollerz, HVDC Light: a tool for electric power transmission to distant loads, VII Sepope Conf. Proc., (1998).

[17] G. Asplund, K. Eriksson and K. Svensson, DC transmission based on voltage source converters, CIGRE SC14 Colloquium, South Africa Proc., (1997) pp. 1-7.

[18] G. Asplund, Application of HVDC Light to power system enhancement, IEEE Power Engineering Society Winter Meeting Conf. Proc., 4 (2000) 2498-2503.

[19] K. Eriksson, Operational experience of HVDC Light, IEE International Conf. on AC-DC Power Transmission Proc., (2001) 205-210.

[20] A. Petersson and A. Edris, Dynamic performance of the Eagle Pass back-to-back HVDC Light tie, IEE International Conf. on AC-DC Power Transmission Proc., (2001) 220-225.

[21] U. Axelsson, A. Holm, C. Liljegren, M. Aberg, K. Eriksson and O. Tollerz, The Gotland HVDC Light project-experiences from trial and commercial operation, 16thIEE International Conf.and Exhibition on Electricity Distribution Proc. (2001).

[22] T. F. Nestli, L. Stendius, M. J. Joahansson, A. Abrahamsson and P. C. Kjaer, Powering Troll with new technology, ABB Review, 2 (2003) 15-19.

[23] L. Stendius and P. Jones, The challenge of offshore power system construction-bringing power successfully to Troll A, one of the world's largest oil and gas platform, IEE International Conf. on AC-DC Power Transmission Proc., (2006) 75-78.

[24] S. G. Johansson, L. Carlsson and G. Russberg, Explore the power of HVDC Light a web based system interaction tutorial, IEEE Power Systems Conf. and Exposition Proc., 2 (2004) 839-842.

[25] B. Andersen and C. Barker, A new era in HVDC?, IEE

Review, 46 (2000) 33-39.
[26] B. Jacobson, Y. J. Hafner, P. Rey, G. Asplund, M. Jeroense, A. Gustafsson, and M. Bergkvist, HVDC with voltage source converters and extruded cables for up to ±300 kV and 1000 MW, CIGRE Conf. Proc. (2006).
[27] A. Hyttinen, J. O. Lamell, and T. F. Nestli, New application of voltage source converter (VSC) HVDC to be installed on the gas platform troll A, CGRE Conf. Proc. (2004).
[28] Y. J. Hafner, M. Hyttinen, and B. Paajarvi, On the short circuit current contribution of HVDC Light, IEEE/PES T&D 2002 Asia Pacific Proc. (2002).
[29] L. Weimers, HVDC Light: A new technology for a better environment, IEEE Power Engineering Review, 18 (1998)19 20.
[30] A. S. Cook, M. Wyckmans, L. Weimers, and K. Eriksson, Network interconnection using HVDC Light, XV EXPO-SNPTEE Conference (1999).
[31] P. C. Krause, O. Wasynczuk, and S. D. Sudhoff, Analysis of Electric Machinery and Drive Systems, John Wiley & Sons Inc., New Jersey, 2002.
[32] T. Ackermann, Wind Power in Power Systems, John Wiley & Sons, Ltd., UK, 2005.
[33] Hee-Sang Ko, Gi-Gab Yoon, and Won-Pyo Hong, Active Use of DFIG-Based Variable-Speed Wind-Turbine for Voltage Regulation at a Remote Location, IEEE Trans. on Power System, 22 (2007) 1916-1925.

This work was supported by National Research Foundation of Korea Grant funded by the Korean Government(20110018632) & the Research Fund of the Korea Institute of Energy Research (KIER).

Biography

Hong-Woo Kim

Hong-Woo Kimwas born in 1962. He received his M.S. degree in Energy Systems Engineering from Sunggyun University, Suwon, Korea, in 1999, and has been a Ph.D. candidate in Electrical Engineering at Chungbuk National University, Cheongju, Korea since 2005. He has been a senior engineer in the wind energy center at the Korea Institute of Energy Research (KIER), Daejeon, Korea since 1990.

Suk-Whan Ko

Suk-Whan Ko was born in 1975. He received his B.S. degree in Electrical Engineering from Kongju National University, Kongju, Korea, in 1998, his M.S. degree in Electrical Engineering from Kongju National University, in 2004, and has been a Ph.D. candidate in Electrical Engineering at Kongju National University since 2009. He has been a senior engineer in the wind energy center at the Korea Institute of Energy Research (KIER), Daejeon, Korea since 2002.

Hae-Joon An

Hae-Joon An was born in 1979. He received his M.S. degree in Electrical Engineering from Dongguk University, Seoul, Korea in 2007, and has been a Ph.D. candidate in Electrical Engineering at Korea University, Seoul, Korea since 2008. He has been a researcher in the wind energy center at the Korea Institute of Energy Research (KIER), Daejeon, Korea since 2007. His research interests include wind power generation, power systems voltage and transient stability.

Gil-Soo Jang

Gil-SooJang was born in 1967. He received his B.S. and M.S. degree from Korea University, Seoul, Korea. He received his Ph. D. degree from Iowa State University in 1997. He worked in the Electrical and Computer Engineering Department at Iowa State University as a Visiting Scientist for one year and at the Korea Electric Power Research Institute as a researcher for two years. He is presently a Professor of the School of Electrical Engineering at Korea University. His research interests include power quality and power system control.

Hee-Sang Ko

Hee-Sang Ko was born in 1969. He received his B.S. degree in Electrical Engineering from Cheju National University, Jeju, Korea, in 1996, his M.Sc. degree in Electrical Engineering from Pennsylvania State University, University Park, USA, in 2000, and his Ph.D. in Electrical and Computer Engineering from the University of British Columbia, Vancouver, Canada, in 2006. He is a researcher in the cooperative planning team at Samsung Heavy Industries Company, Geoje, Korea. His research interests include wind power generation, power system voltage and transient stability, data processing for power system security analysis, electricity market analysis, and system identification.